Regulation of DNA damage responses and cell cycle progression by hMOB2.

Article (Accepted Version)

Cellular Signalling xxx (2014) xxx–xxx

Contents lists available at ScienceDirect

Cellular Signalling

journal homepage: www.elsevier.com/locate/cellsig

Regulation of DNA damage responses and cell cycle progression by hMOB2

Valenti Gomez [a], Ramazan Gundogdu [a], Marta Gomez [a], Lily Hoa [a], Neelam Panchal [a], Mark O'Driscoll [b], Alexander Hergovich [a,*]

[a] UCL Cancer Institute, University College London, WC1E 6BT, London, United Kingdom
[b] Genome Damage and Stability Centre, University of Sussex, BN1 9RH, Brighton, United Kingdom

ARTICLE INFO

Article history:
Received 17 September 2014
Received in revised form 3 November 2014
Accepted 14 November 2014
Available online xxxx

Keywords:
DNA damage response signalling
Mps one binder 2
Cell cycle progression
p53 tumour suppressor protein
Cell cycle checkpoint activation
MRE11–RAD50–NBS1 protein complex

ABSTRACT

Mps one binder proteins (MOBs) are conserved regulators of essential signalling pathways. Biochemically, human MOB2 (hMOB2) can inhibit NDR kinases by competing with hMOB1 for binding to NDRs. However, biological roles of hMOB2 have remained enigmatic. Here, we describe novel functions of hMOB2 in the DNA damage response (DDR) and cell cycle regulation. hMOB2 promotes DDR signalling, cell survival and cell cycle arrest after exogenously induced DNA damage. Under normal growth conditions in the absence of exogenously induced DNA damage hMOB2 plays a role in preventing the accumulation of endogenous DNA damage and a subsequent p53/p21-dependent G1/S cell cycle arrest. Unexpectedly, these molecular and cellular phenotypes are not observed upon NDR manipulations, indicating that hMOB2 performs these functions independent of NDR signalling. Thus, to gain mechanistic insight, we screened for novel binding partners of hMOB2, revealing that hMOB2 interacts with RAD50, facilitating the recruitment of the MRE11–RAD50–NBS1 (MRN) DNA damage sensor complex and activated ATM to DNA damaged chromatin. Taken together, we conclude that hMOB2 supports the DDR and cell cycle progression.

1. Introduction

The family of Mps one binder (MOB) proteins is highly conserved from yeast to humans [1]. Yeast expresses two MOB proteins, the *Drosophila* genome encodes three different MOBs, termed dMOBs, and mammalian genomes encode at least six different members (MOB1A, MOB1B, MOB2, MOB3A, MOB3B, MOB3C), indicating a functional diversification of MOBs from unicellular to complex multicellular organisms [1]. In yeast, Mob1p and Mob2p are required for mitotic exit and cell morphogenesis through regulation of the conserved NDR/LATS kinases Dbf2p and Cbk1p [2–4]. In flies dMOB1 (also termed Mats) functions as an essential tumour suppressor together with Warts/Lats kinase [5–7], while dMOB2 has reported roles in neuromuscular junctions [8] and photoreceptors [9] that might be regulated by the association of dMOB2 with Tricornered [10], the fly counterpart of human NDR kinases [11]. dMOB1 and dMOB3 can also genetically interact with Tricornered [10]. However, the biological roles of dMOB3 are yet to be defined in flies.

In mammals, the tumour suppressive role of MOB1 as a LATS regulator is conserved [5,12,13]. Significantly, MOB1-deficient mice [14] develop a broader range of tumours as reported for loss of LATS kinases [5], suggesting that MOB1 performs important biological functions independent of LATS signalling. Perhaps this involves the interaction of MOB1 with NDR kinases, since MOB1 can interact with NDR kinases through a domain conserved between LATS and NDR kinases [13,15]. In contrast, although MOB2 binds to this same domain, MOB2 can only associate with NDR, but not with LATS kinases [16–18]. Currently, NDR kinases are the only reported binding partners of hMOB2 [1]. hMOB2 competes with hMOB1 for NDR binding [18], hence the hMOB1/NDR complex is associated with increased NDR activity [19], while hMOB2 binding to NDR blocks NDR activation [18]. In contrast, hMOB3 neither associates with NDR nor LATS [18], but rather interacts with the pro-apoptotic kinase MST1, thereby negatively regulating apoptotic signalling in glioblastoma multiforme [20]. Therefore, mammalian MOB1 and MOB3 have been attributed tumour suppressive or oncogenic roles, respectively. However, although the human *MOB2* gene appears to display loss of heterozygosity (LOH) in more than 50% of bladder, cervical, and ovarian carcinomas (The Cancer Genome Atlas, TCGA) [21], any defined physiological cancer-related functions of mammalian MOB2 have yet to be described. So far, it has only been reported that MOB2 can contribute to morphological changes in murine neurites and rat astrocytes [22,23].

Abbreviations: MOB, Mps one binder; NDR, Nuclear Dbf2-related; LATS, Large tumour suppressor; DDR, DNA damage response; MRN, MRE11-RAD50-NBS1; IR, Ionizing radiation; DSB, DNA double strand break; ATM, Ataxia telangiectasia mutated; PIF, PDK1-interacting fragment.

* Corresponding author at: UCL Cancer Institute, University College London, 72 Huntley Street, WC1E 6DD, London, United Kingdom. Tel.: +44 20 7679 0723.
E-mail address: a.hergovich@ucl.ac.uk (A. Hergovich).

http://dx.doi.org/10.1016/j.cellsig.2014.11.016
0898-6568/

A recent genome wide screen for novel players in the DNA damage response (DDR) identified hMOB2 (also termed HCCA2) as one of many candidates awaiting validation of their potential role in the DDR [24]. To date, direct or indirect functions in the DDR have not been described for any MOB2 family member. Therefore, considering that the DDR is critical to maintain genomic integrity and to prevent ageing

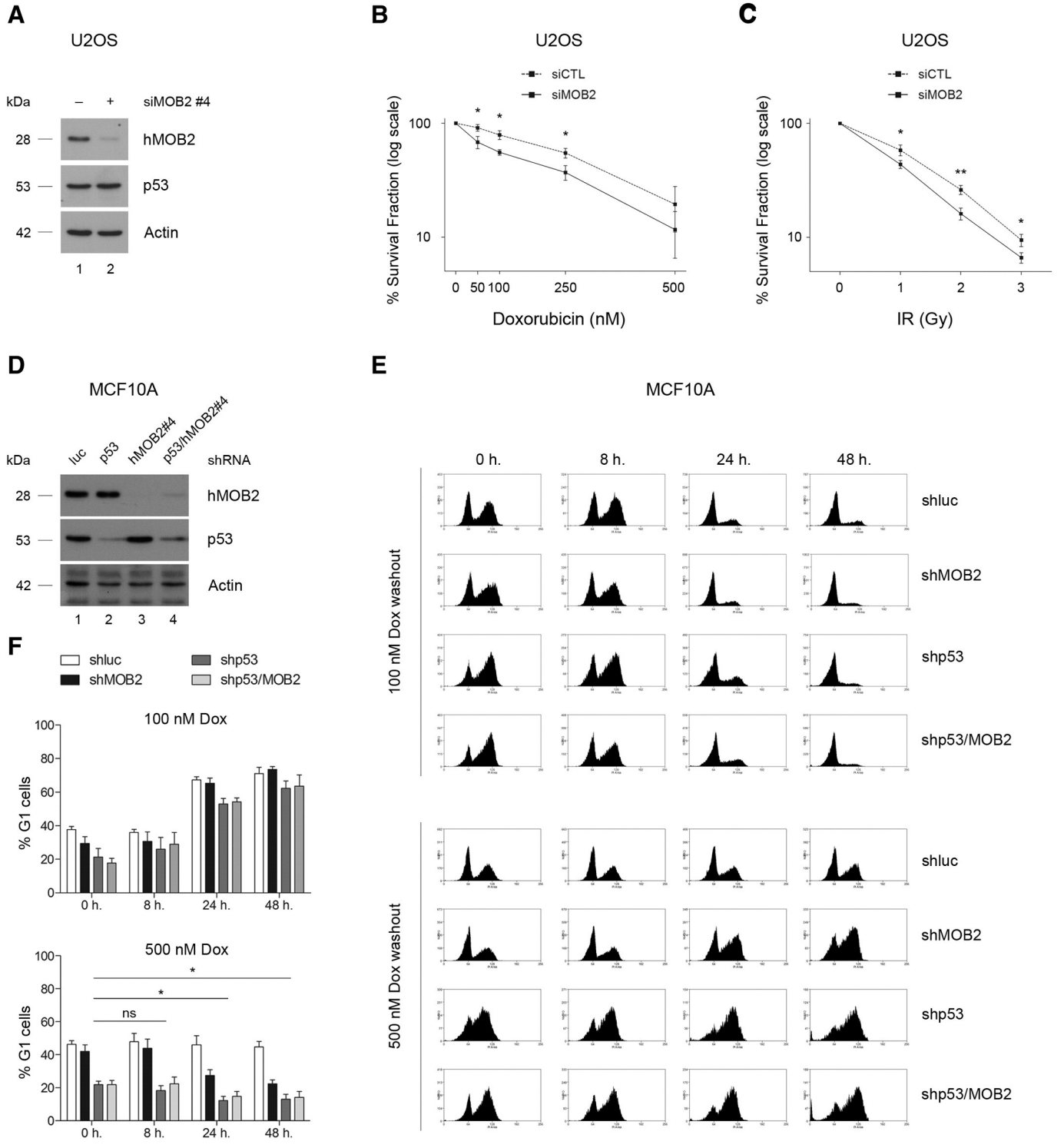

Fig. 1. hMOB2 promotes cell survival and G1/S cell cycle arrest in response to exogenously induced DNA damage. (A) Immunoblotting with indicated antibodies of U2-OS cell lysates from cells transiently transfected for 24 h with indicated siRNAs. (B, C) Clonogenic survival of U2-OS cells upon hMOB2 knockdown (siMOB2) compared with controls (siCTL) in response to doxorubicin or ionising radiation (IR). Quantifications are shown as percentage of colonies formed after treatment with indicated doses (n = 4). Results were corrected according to plating efficiencies of the corresponding untreated controls. *P*-values are: 50 nM = 0.037, 100 nM = 0.018, 250 nM = 0.029, 500 nM = 0.231; 1 Gy = 0.039, 2 Gy = 0.005, 3 Gy = 0.035. (D) Immunoblotting with indicated antibodies of MCF10A cell lysates from pSuper.retro.puro infected cells expressing indicated shRNAs. (E) Cell cycle analysis of MCF10A cell pools treated with indicated doxorubicin doses, before release in drug-free medium for indicated time points. Representative time courses are shown. (F) Histograms showing percentages of MCF10A cells in the G1 cell cycle phase (n = 3). Control (shLuc), hMOB2-depleted (shMOB2), p53-depleted (shp53), and hMOB2/p53 co-depleted (shp53/MOB2) cells were compared. *P*-values are: 8 h = 0.397 (ns, not significant), 24 h = 0.027, 48 h = 0.011.

Please cite this article as: V. Gomez, et al., Cell. Signal. (2014), http://dx.doi.org/10.1016/j.cellsig.2014.11.016

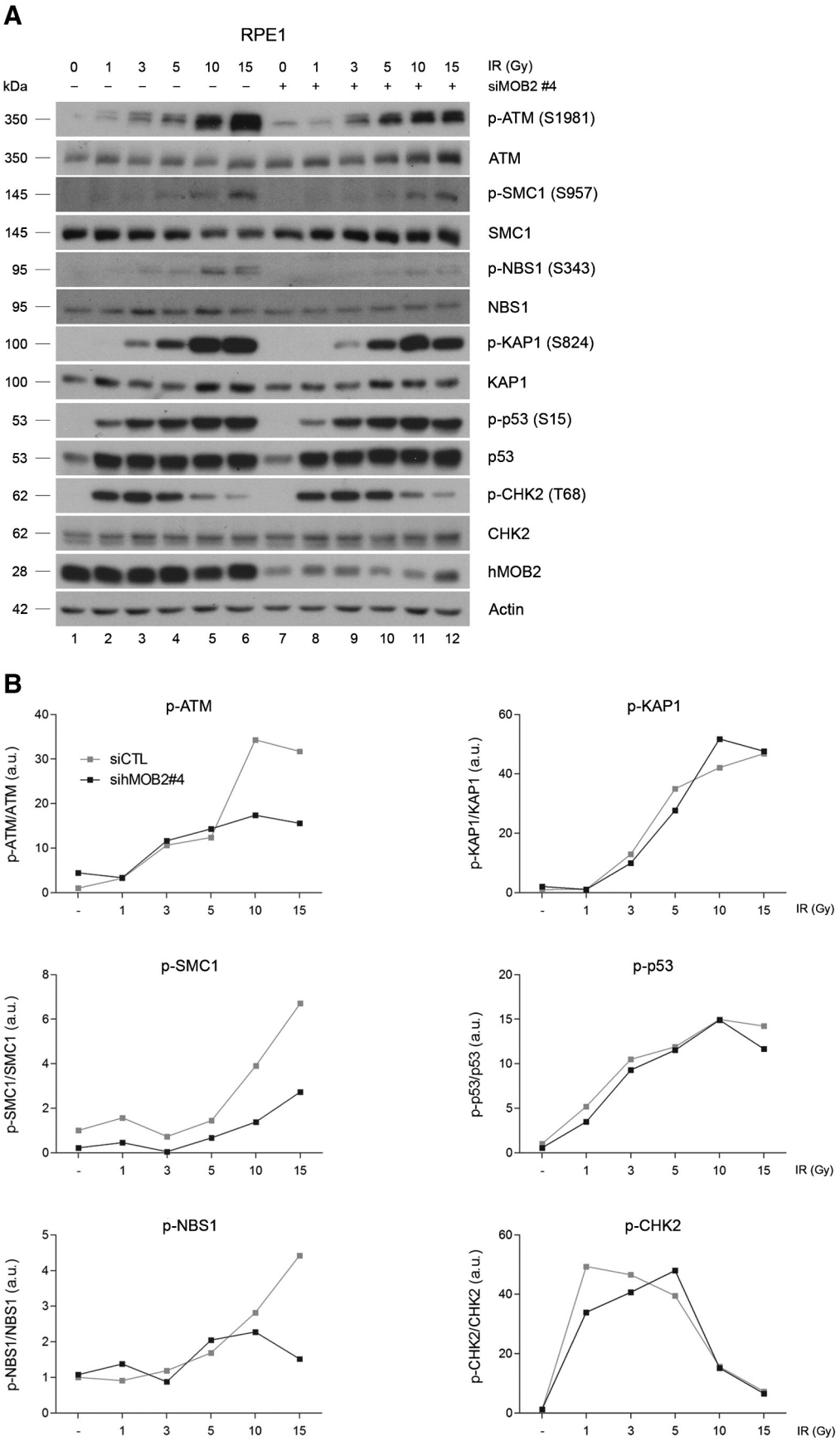

Fig. 2. hMOB2 supports IR-induced ATM-NBS1-SMC1 signalling. (A) Phosphorylation of ATM and ATM substrates analysed by immunoblotting with indicated antibodies of RPE1 cell lysates from cells transiently transfected for 24 h with indicated siRNAs (−, siCTL; +, siMOB2). Cells were treated with indicated ionising radiation (IR) doses, before processing for immunoblotting. (B) Graphs showing the kinetics of ATM activation as judged by Ser1981 auto-phosphorylation and substrate phosphorylations by ATM obtained by densitometry quantification of Western blots shown in A (phosphorylated/total proteins).

Please cite this article as: V. Gomez, et al., Cell. Signal. (2014), http://dx.doi.org/10.1016/j.cellsig.2014.11.016

and tumourigenesis [25], we decided to investigate on the cellular and molecular level whether hMOB2 is a DDR protein. Here, we show that hMOB2 promotes cell survival, cell cycle checkpoint activation, and DDR signalling upon exogenously induced DNA damage. Under normal growth conditions in the absence of exogenously induced DNA damage hMOB2 loss causes the accumulation of DNA damage, triggering a p53/p21-dependent G1/S cell cycle arrest not phenocopied by NDR manipulations. Thus, to gain mechanistic insights, we screened for novel binding partners of hMOB2, discovering that hMOB2 interacts with RAD50, a key component of the essential MRE11–RAD50–NBS1 (MRN) DNA damage sensor complex [26–28]. hMOB2 supports the recruitment of MRN and activated ATM to DNA damaged chromatin, thereby providing the first mechanistic insight into why hMOB2 can play a role in DDR signalling, cell survival, and cell cycle checkpoints after DNA damage induction.

2. Materials and methods

2.1. Cell culture, chemicals, drug treatments, and transfections

RPE1-hTert, COS-7, PT67 and U2-OS cells were maintained in DMEM supplemented with 10% foetal calf serum (FCS). BJ-hTert fibroblasts were grown in DMEM:Medium199 (4:1) supplemented with 10% FCS and gentamicin (50 μg/ml). MCF10A cells were maintained as described [29]. Blasticidin, zeocin, puromycin (Invivogen), and G418 (PAA Laboratories) were used as reported [30]. Exponentially growing cells were plated at a consistent confluence and transfected with siRNAs and plasmids using Fugene 6 (Promega), Lipofectamine RNAiMax (Invitrogen), or Lipofectamine 2000 (Invitrogen) according to the manufacturer's instructions. Tetracycline (Sigma) was used as described [30]. Doxorubicin (Sigma) was added as indicated. For drug washout experiments, cells were washed three times with complete media without drug and allowed to recover in complete medium without drug. All siRNAs were from Qiagen and sequences are available upon request.

2.2. Generation of stable cell lines and IR treatments of cells

Tetracycline-inducible (Tet-on) cell lines were generated and maintained as described [30]. Briefly, RPE1 hTert Tet-on cells [30] were transfected with pTER constructs [31] expressing shRNAs against NDR1 or hMOB2, or pT-Rex-HA-NDR1-PIF plasmid, and selected as described [30]. Retroviral pools using pMKO.1 puro, pSuper.retro.puro, or pLXSN plasmids were generated as reported [32]. For IR treatments, cells were seeded at fixed densities, followed by irradiation with indicated doses at a rate of 5 Gy/min (215 kV, 12.0 mA, 1.0 mm Al filter) using an AGO HS 320/250 X-ray machine (AGO X-ray Ltd.) equipped with a NDI-321 stationary anode X-ray tube (Varian), and then processed for immunoblotting, clonogenic, or comet assays as described below.

2.3. Yeast two-hybrid (Y2H) screen

To identify novel direct hMOB2 binding partners, a normalised universal human tissue cDNA library was screened using pLexA-N-hMOB2(full-length) as bait. The complexity of the pGADT7-recAB based cDNA library was 2.8 × 10E6 with an average insert size of 1.58 kb. Screening of 1 × 10E6 transformants yielded 59 bait dependent hits, resulting in the identification of total 28 putative interactors. Only four novel binding partners of hMOB2 were identified at least twice (RAD50, UBR5, KPNB1, and KIAA0226L). All nine hits for UBR5 were out of frame and identified the HECT domain of UBR5 as potential interaction site, while all four hits for RAD50 were in frame (see Supplementary Table S1). The Y2H screen was performed by Dualsystems Biotech AG (Zurich, Switzerland).

2.4. Immunoblotting, immunoprecipitations, chromatin isolation, and densitometry analysis

Immunoblotting and co-immunoprecipitation (co-IP) were done as described [32,33]. For chromatin–cytosol separations, cells were harvested with ice-cold PBS, centrifuged for 2 min at 1000 ×*g* at 4 °C, and resuspended in buffer A (10 mM Pipes, 100 mM NaCl, 300 mM sucrose, 3 mM MgCl2, 5 mM, EDTA, 1 mM EGTA, 50 mM NaF, 0.1 mM Na_3VO_4, 0.1% Triton X-100, 1 mM benzamidine, 4 μM leupeptin, 0.5 mM PMSF and 1 mM DTT at pH 6.8). Lysates were incubated for 10 min and then centrifuged for 5 min at 1300 ×*g* at 4 °C. Supernatants were collected as cytosolic fraction. Pellets were washed once with buffer A, lysed for 10 min at 4 °C in buffer B (3 mM EDTA, 0.2 mM EGTA, 1 mM benzamidine, 4 μM leupeptin, 0.5 mM PMSF and 1 mM DTT at pH 8.0), followed by centrifugation for 5 min at 1700 ×*g* at 4 °C. Supernatants (soluble nuclear fraction) were discarded. Pellets (insoluble chromatin fraction) were washed once with buffer B, resuspended in Laemmli buffer and fragmented using a 26G Microlance G needle (BD). Equal volumes of fractions were analyzed by immunoblotting. Densitometry analysis of immunoblots was performed using the ImageJ software (NIH).

2.5. Antibodies (generation and sources)

Rat polyclonal anti-hMOB2 antibodies were raised against purified, bacterially produced full-length hMOB2 fused C-terminally to GST protein. Rat injections/bleed collections were done by Eurogentec. Anti-protein antibody was purified by pre-absorbing the bleeds against 10 mg of immobilised GST and then binding to 10 mg of maltose binding protein (MBP)-hMOB2 coupled to amylose beads (New England Biolabs). Antibodies were eluted with 0.2 M glycine (pH 2.5). Anti-HA 12CA5, anti-myc 9E10 and anti-NDR2 antibodies have been described [34,35]. All antibodies are listed in Supplementary Table S2.

2.6. Immunofluorescence microscopy

Cells were processed for immunofluorescence as defined [32,33]. Images were acquired with an ApoTome fluorescence microscope (Zeiss) and processed with AxioVision AxioVS40 V4.8.1.0 (Zeiss) and Photoshop CS5 (Adobe Systems Inc.).

2.7. FACS cell cycle and cell proliferation analyses

For FACS analysis of DNA content cells were processed as defined elsewhere [32], before analysis using a CyAn ADP Flow Cytometer (Beckman Coulter). Cell cycle profiles were analyzed with Summit (Beckman Coulter) and FlowJo (Tree Star) softwares. For cell proliferation analysis, cells were seeded at defined densities in triplicates. For experiments involving Tet-on cell lines, fresh tetracycline was added the day of seeding. At indicated time points, the number of viable cells was determined by trypan blue exclusion using the automated ViCell-XR cell counter (Beckman Coulter).

2.8. Comet assays

Single cell gel electrophoresis (comet) assays were performed as described [36]. After electrophoresis individual cells were visualised using an inverted microscope (Nikon) and analysed using Komet Analysis software 4.02 (Andor Technology). Per sample/time point/experiment at least 100 cells were randomly selected from duplicate slides and individual DNA damage levels were determined.

2.9. Clonogenic survival assays

Clonogenic assays were performed as described [37]. Briefly, cells were seeded at predetermined densities in six-well plates and allowed

Please cite this article as: V. Gomez, et al., Cell. Signal. (2014), http://dx.doi.org/10.1016/j.cellsig.2014.11.016

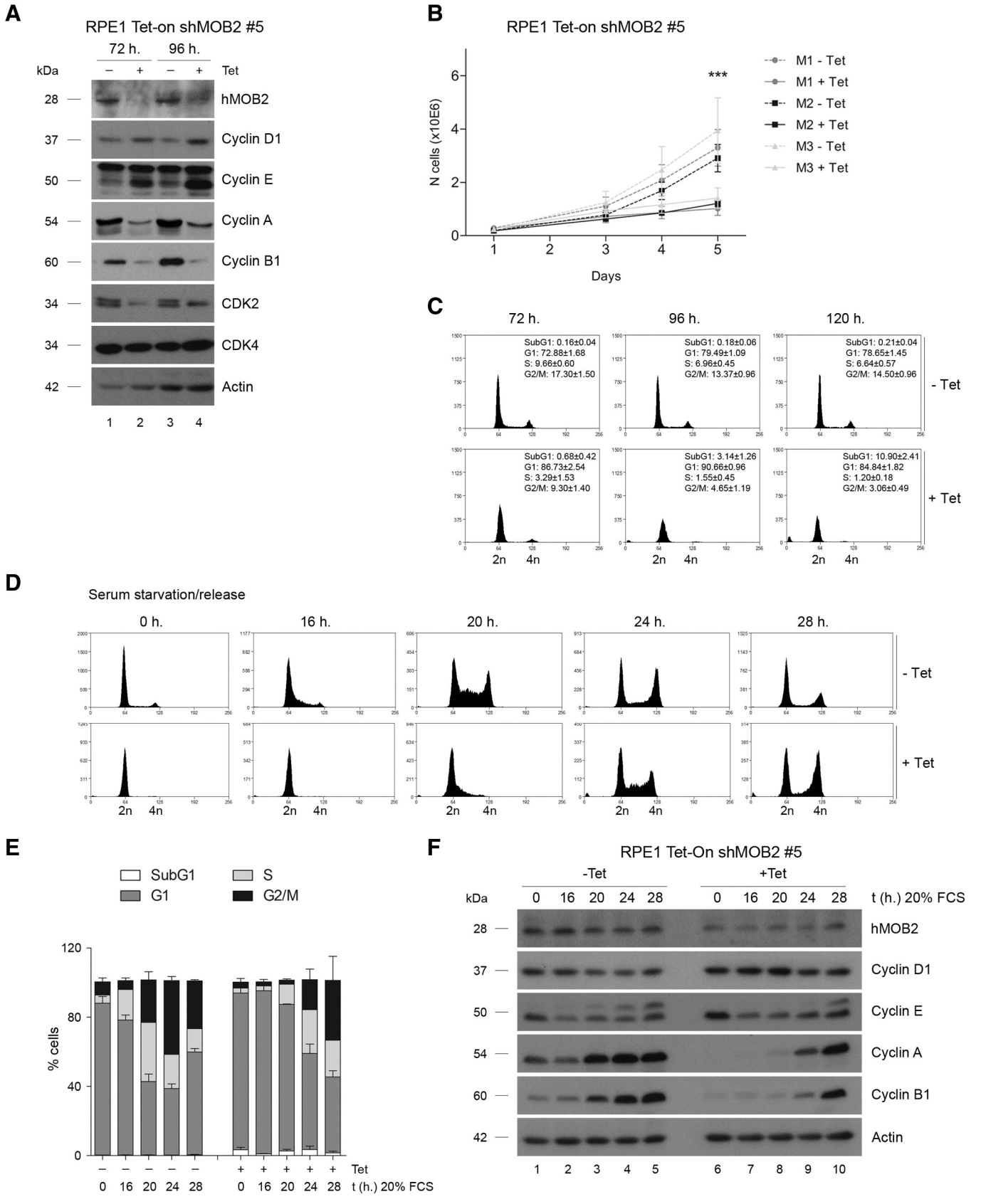

Fig. 3. hMOB2 is required for cell cycle progression. (A) Immunoblotting with indicated antibodies of RPE1 Tet-on shMOB2 cell lysates after incubation of cells with (+Tet) or without (−Tet) tetracycline as indicated. (B) Proliferation rates of three independent RPE1 Tet-on shMOB2 clones (n = 3; *P*-value = 0.0012). (C) Cell cycle analyses of RPE1 Tet-on shMOB2 cells at indicated time points with (+Tet) or without (−Tet) of tetracycline. Percentages of cells in each cell cycle phase are shown (n = 3). (D) RPE1 Tet-on shMOB2 cells with (+Tet) or without (−Tet) tetracycline were serum starved for 72 h, washed twice, released in medium containing 20% FCS, and processed for cell cycle analysis at indicated time points. (E) Histograms showing the percentage of synchronised cells in each cell cycle phase (n = 3). (F) Immunoblotting with indicated antibodies of cell lysates obtained from synchronised cell cultures described in D.

to adhere for 24 h, before being irradiated or drug treated as indicated, followed by three media washes. Cells were replenished with fresh complete medium every 3 days until colony size reached more than 50 cells per colony. Then cells were fixed with MeOH/acidic acid (3:1) solution for 5 min, followed by staining with 0.5% crystal violet (Sigma) for 15 min. The surviving fraction was calculated using

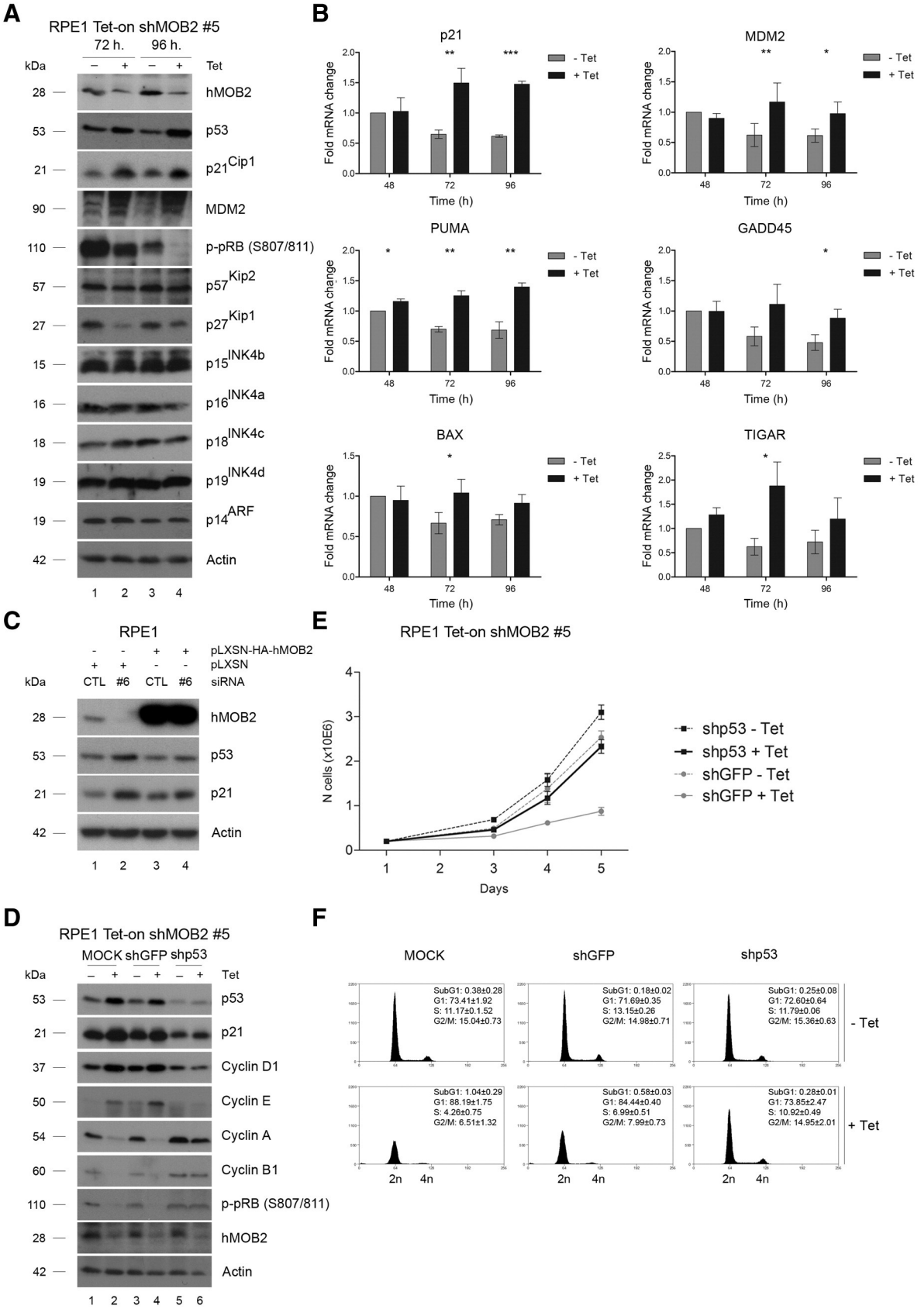

the plating efficiencies of the corresponding non-treated controls as reference.

2.10. Construction of plasmids

hMOB2 and NDR1/2 cDNA and shRNA plasmids were described [18,19,32]. pT-Rex-HA-NDR1-PIF was generated by inserting HA-NDR1-PIF [38] into pT-Rex-DEST30 (Invitrogen) using Gateway technology (Invitrogen). The RAD50 cDNA was amplified by PCR and subcloned into pcDNA3_HA using *Bam*HI and *Xho*I. pCMV-FLAG-UBR5 full-length was kindly provided by R. Sutherland (Garvan Institute of Medical Research, Sydney, Australia), and used as a template to amplify the HECT domain (residues 2501 to 2799), which was subcloned into pcDNA3_HA using *Bam*HI and *Xho*I. pMKO.1 puro shGFP (10675) and pMKO.1 puro shp53 (10672) were from Addgene. To generate pSuper.retro.puro_shLUC (luciferase control), pSuper.retro.puro_shp53#2, pSuper.retro.puro_shMOB2#4, and pSuper.retro.puro_shMOB2#6 vectors that express shRNAs against human p53 and hMOB2, the following oligonucleotide pairs were inserted into pSuper.retro.puro (Oligoengine) using *Bgl*II and *Hind*III: 5′-GATCCCCGTACGCGGAATACTTCGATTCAAGAGATCGAAGTATTCCGCGTACGTTTTTGGAAA-3′ and 5′-AGCTTTTCCAAAAACGTACGCGGAATACTTCG ATCTCTTGAATCGAAGTATTCCGCGTACGGG-3′ targeting firefly luciferase; 5′-GATCCCGACTCCAGTGGTAATCTACTTCAAGAGAGTAGATTACCACTGGAGTCTTTTTGGAAA-3′ and 5′-AGCTTTTCCAAAAAGACTCCAGTGGTAATCTACTCTCTTGAAGTAGATTACCACTGGAGTCGG-3′ for targeting p53; 5′-GATCCCGGAGAGACGTGTCAGACGATTCAAGAGATCGTCTGACACGTCTCTCCTTTTTGGAAA-3′ and 5′-AGCTTTTCCAAAAAGGAGAGACGTGTCAGACGATCTCTTGAATCGTCTGACACG TCTCTCCGG-3′, or 5′-GATCCCGCGTGCCGTTTGTAGAGAGTTCAAGAG ACTCTCTACAAACGGCACGCTTTTTGGAAA-3′ and 5′-AGCTTTTCCAAAAAG CGTGCCGTTTGTAGAGAGTCTCTTGAACTCTCTACAAACGGCACGCGG-3′ for targeting hMOB2. For siRNA rescue experiments, HA-tagged hMOB2 cDNA was subcloned into pLXSN (Clontech) using *Hpa*I and *Xho*I. All constructs were confirmed by sequence analysis. Further details of the generation of constructs and sequences of primers are available upon request.

2.11. RNA isolation, cDNA synthesis, and real-time quantitative PCR gene expression analysis

Total RNA was extracted using Trizol Reagent (Life Technologies) following the manufacturer's protocol. RNA concentration and integrity was determined using a NanoDrop 1000 spectrophotometer (Thermo Scientific). cDNA synthesis was performed using iScript One-Step RT-PCR Kit (Bio-Rad). qPCR was carried out using validated qPCR primers (Qiagen) and the QuantiTect SYBR Green PCR Kit (Bio-Rad) using the Mastercycler ep realplex (Eppendorf). 18S rRNA served as internal control for standardisation.

2.12. Statistical analysis

Graphics and statistical analyses were carried out using the GraphPad Prism software. Data are presented as mean ± s.e.m., unless stated otherwise. The significance of differences between the means or the population distributions was determined using the two-way ANOVA test (for proliferation analysis), or one-tailed unpaired Student's *t*-test (for RTqPCR, γH2A.X/53BP1, comet experiments, clonogenic survival assays, and G1/S cell cycle checkpoint experiments). For all tests, differences were considered statistically significant when *P* values were below 0.05 (*), 0.01 (**), or 0.001 (***), respectively. *P*-values are indicated in the corresponding figure legends.

3. Results

3.1. hMOB2 promotes cell survival and G1/S cell cycle arrest after DNA damage induction

Since hMOB2 (HCCA2) might represent a novel DDR protein [24], we tested whether hMOB2 is required for cell survival of cells after exposure to DNA damage. We employed U2-OS cells, as they are routinely used for clonogenic cell survival assays in the context of DNA damaging agents [39]. To induce DNA damage exogenously, cells were treated with doxorubicin or ionising radiation (IR), both of which can induce DNA double strand break (DSB) and are routinely used in chemotherapy regimens [40]. To circumvent effects due to possibly altered cell cycle progression, we employed acute (1 h) doxorubicin treatments of cells 24 h after siRNA transfection (Fig. 1A). hMOB2 depletion caused significantly increased drug- and radio-sensitivities (Fig. 1B and C), revealing that hMOB2 contributes to cell survival following exposure to doxorubicin or IR. The results reported in the genome wide DDR screen [24] proposed that hMOB2 contributes to mitomycin C sensitivity. In full support of this screening result [24], we observed that depletion of hMOB2 in U2-OS cells also causes increased sensitivity to the chemotherapeutic agent mitomycin C (data not shown). Taken together, these findings suggest that hMOB2 knockdown is sufficient to cause increased sensitivities towards three commonly used DNA damaging therapeutics.

Elledge and colleagues further showed in their DDR screen that hMOB2 knockdown cells have impaired activation of the IR-induced G2/M cell cycle checkpoint [24]. We therefore asked whether other DDR cell cycle checkpoints are also dependent on hMOB2. To address the p53-regulated G1/S checkpoint we chose to employ a previously reported approach using untransformed human MCF10A cells [41]. MCF10A cells were chronically (stably) depleted of hMOB2, p53 or both together (Fig. 1D). DDR-mediated cell cycle perturbations were assessed at selected time points after treatment and washout of indicated doxorubicin doses (Fig. 1E and F). As expected [42], control cells arrested mainly at the G1/S and G2/M cell cycle phases, while p53-depleted cells arrested only at the G2/M checkpoint. hMOB2-depleted cells initially arrested at G1/S similar to controls. Upon washout of 100 nM doxorubicin, controls and hMOB2-depleted cells rapidly resumed cell cycle progression. However, upon washout of 500 nM doxorubicin hMOB2-depleted cells quickly resumed G1/S cell cycle progression in contrast to controls (Fig. 1F, bottom panel), indicating a defective G1/S checkpoint in hMOB2-depleted cells upon exposure to high DNA damage levels. Collectively, these findings together with the data by Cotta-Ramusino et al. [24] suggest that upon exogenously induced DNA damage hMOB2 functions in promoting cell survival and cell cycle checkpoints, two hallmarks of the DDR.

3.2. hMOB2 is required for normal ATM–NBS1–SMC1 signalling in the DDR

Next, we addressed a third hallmark of the DDR in the context of hMOB2 manipulation. In response to DNA damage, the MRN DNA

Fig. 4. hMOB2 depletion results in a p53-dependent G1/S cell cycle arrest. (A) Immunoblotting with indicated antibodies of RPE1 Tet-on shMOB2 cell lysates from cells incubated with (+Tet) or without (−Tet) tetracycline as indicated. (B) Quantitative real time PCR analysis of indicated p53 target genes in RPE1 Tet-on shMOB2 cells at indicated time points in the presence (black bars) or absence (gray bars) of tetracycline (n = 3). *P*-values are: p21, 72 h = 5.5E−03, 96 h = 5.2E−05; MDM2, 72 h = 1.3E−03, 96 h = 0.018; PUMA, 48 h = 0.033, 72 h = 1.7E−03, 96 h = 4.4E−03; GADD45, 96 h = 0.026; BAX, 72 h = 0.047; TIGAR, 72 h = 0.025. (C) Immunoblotting of RPE1 cell lysates from cells stably expressing empty vector (pLXSN) or siRNA-resistant hMOB2 (pLXSN-HA-hMOB2) transfected with indicated siRNAs (CTL, control; #6, siRNA targeting the 3′UTR of hMOB2). (D) Immunoblotting of RPE1 Tet-on shMOB2 cell lysates from cells infected with indicated plasmids. Cell pools were analysed after 4 days with (+Tet) or without (−Tet) tetracycline. (E) Cell proliferation rates of cell pools described in D were analysed in the presence (+Tet) or absence (−Tet) of tetracycline (n = 3). (F) Cell cycle analyses of cell pools after 4 days in the presence (+Tet) or absence (−Tet) of tetracycline. Percentages of cells in each cell cycle phase are shown (n = 3).

Please cite this article as: V. Gomez, et al., Cell. Signal. (2014), http://dx.doi.org/10.1016/j.cellsig.2014.11.016

damage sensor and other essential factors, such as PARP and Ku70/80, bind rapidly to damaged DNA in order to activate a co-ordinated programme of events [43], which involves MRN-mediated recruitment of the ataxia-telangiectasia mutated (ATM) kinase to DSBs [26–28]. Once activated by autophosphorylation [44], the central DDR protein kinase ATM phosphorylates many substrates involved in DDR signalling [45].

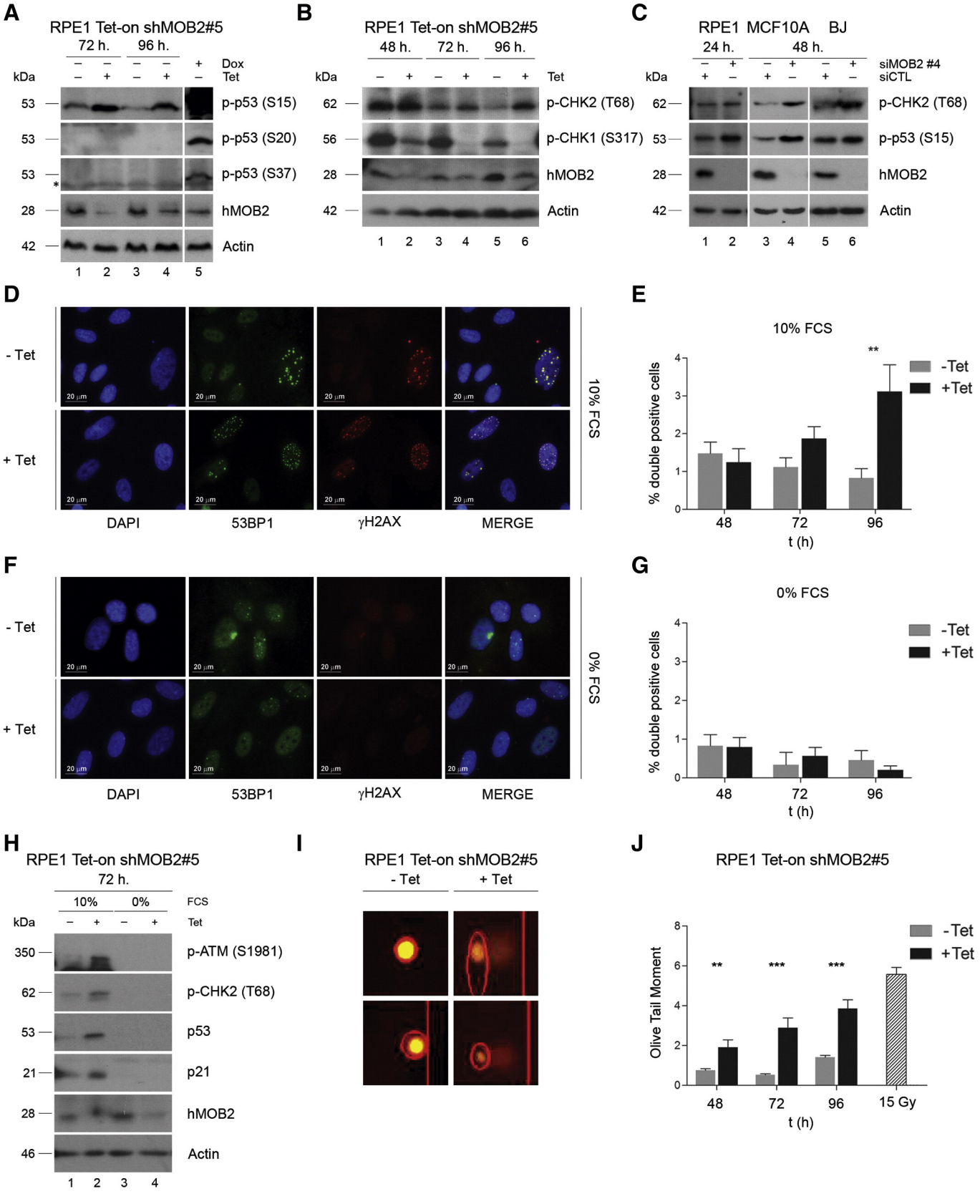

Activated ATM phosphorylates effectors, such as p53, CHK2, and KAP1, as well as the MRN component NBS1 to create a positive feedback loop maintaining ATM activity [45]. ATM further phosphorylates SMC1, an event required for cell survival in response to DNA damage [46–48]. Therefore, to study these multiple branches of DDR signalling, IR-induced phosphorylation of ATM and a panel of ATM substrates were compared between controls and hMOB2-knockdown cells 24 h post siRNA transfections (Fig. 2A and B). Intriguingly, this analysis revealed that the IR-induced phosphorylation levels of ATM, SMC1 and NBS1 were significantly altered in hMOB2-depleted cells, while p53, CHK2, and KAP1 phosphorylation was unaffected when compared to controls (Fig. 2A and B). This indicates that hMOB2 is dispensable for some ATM activities, while being required for optimal ATM activation and ATM-mediated phosphorylation of NBS1 and SMC1. Thus, given that hMOB2 is needed for some aspects of DDR signalling, hMOB2 displays another hallmark of a DDR protein. Collectively, our results propose that hMOB2 supports the DDR, since upon DNA damage induction three different hallmarks of the DDR, namely cell survival, cell cycle checkpoint activation, and DDR signalling are impaired in hMOB2-depleted cells.

3.3. hMOB2 is needed to prevent a transient p53/p21-dependent G1/S cell cycle arrest

As the phenotypes described in Figs. 1 and 2 were based on exogenously induced DNA damage, we sought to complement our analysis by examining the role of endogenous hMOB2 in untransformed human cells under normal growth conditions in the absence of exogenously induced DNA damage. Given that cell survival in response to DNA damage relies on proper cell cycle control, we focused on investigating hMOB2 in cell cycle progression. This unbiased approach is crucial, since some essential DDR regulators are cell cycle regulated which can complicate the analyses of cellular and molecular DDR phenotypes. For example, MRN protein, but not mRNA, levels are cell cycle regulated [49], hence any study relating to MRN functionality that does not take cell cycle progression into account is likely to examine a mix of direct and indirect effects. To ensure that our work does not suffer from such shortcomings, we engineered [30] untransformed human RPE1 cells with tetracycline-inducible (Tet-on) hMOB2 depletion in order to study cell cycle progression in consistent knockdown conditions. Significantly, hMOB2 depletion increased the levels of the G1/S markers cyclin D1 and E, while decreasing the S/G2/M markers cyclin A and B1 (Fig. 3A). These changes in cyclin expression were accompanied by impaired cell proliferation upon hMOB2 silencing (Fig. 3B). Analyses of cell cycle profiles revealed that hMOB2-depleted cells displayed a G1/S cell cycle arrest (Fig. 3C). The stable Tet-on system also allowed us to deplete hMOB2 in serum starved cells, prior to addition of serum in order to synchronously release cells from G0/G1 into S-phase. Notably, this approach revealed that synchronised hMOB2-silenced cells displayed a markedly delayed G1/S cell cycle transition (Fig. 3D–F). Collectively, these findings indicate that endogenous hMOB2 is required for normal cell cycle progression.

To define the underlying molecular basis of the G1/S arrest upon hMOB2 depletion, we expanded our analysis of cell cycle regulators (Fig. 4A). We observed activation of the p53–pRB axis [42] through p53 stabilisation and decreased pRB phosphorylation following hMOB2 knockdown (Fig. 4A). Furthermore, p21/Cip1 and Mdm2, two established p53 target genes [50], were elevated at the protein and mRNA levels (Fig. 4A and B). Expression of other p53 target genes was also significantly enhanced (Fig. 4B and Supplementary Fig. S1A). These findings indicate that transcriptionally active p53 is stabilised upon MOB2 silencing. Transfections of three different untransformed human cell lines with three independent siRNAs directed against hMOB2 consistently elevated p53 levels (Supplementary Fig. S1B). Expression of siRNA-resistant hMOB2 interfered with p53 induction upon MOB2 depletion (Fig. 4C), hence rescuing the phenotype caused by RNAi-mediated silencing of hMOB2. Taken together, these approaches rule out the possibility that the stabilisation of active p53 upon hMOB2 depletion is a consequence of RNAi off-target effects.

Sustained p53 stabilisation results in a permanent proliferation arrest through senescence, while pulses of stabilised p53 yield a transient cell cycle arrest [51]. Using increased cell size as senescence marker [52], we found that hMOB2 knockdown does not cause senescence in RPE1 cells (data not shown). Our data rather suggest that hMOB2 silencing triggers a transient p53-dependent arrest, since co-depletion of hMOB2 together with p53 restored normal cell proliferation, abolishing the G1/S cell cycle arrest (Fig. 4D–F). Co-depletion of hMOB2 and p21 resulted in a similar restoration of cell cycle progression in spite of increased p53 levels (Supplementary Fig. S2). Therefore, p53-mediated upregulation of p21 likely underlies the G1/S cell cycle arrest observed upon hMOB2 reduction under normal growth conditions in the absence of exogenously induced DNA damage.

3.4. hMOB2 depletion triggers a DNA damage–ATM–CHK2–p53–p21 cascade

Given that the p53–p21 pathway is a master regulator of the G1/S cell cycle transition in the DDR [50], we were prompted to examine p53 in the context of DDR signalling in hMOB2-depleted cells under normal growth conditions. We hypothesised that a DDR defect due to hMOB2 knockdown could explain why hMOB2-depleted cells displayed a p53-dependent G1/S cell cycle arrest. Possibly hMOB2-depleted cells accumulate unrepaired DNA damage, which can trigger p53 activation. Significantly, upon hMOB2 depletion increased p53 protein levels did not correlate with changes in p53 mRNA expression (Fig. 4A and Supplementary Fig. S1A), while p53 phosphorylation on Ser15 did (Fig. 5A), revealing a possible stabilisation mechanism of p53 [50]. CHK2 phosphorylation on Thr68 was also augmented (Fig. 5B), indicating elevated ATM activity upon hMOB2 knockdown under normal growth conditions. hMOB2 depletion in untransformed human BJ and MCF10A cells by an independent siRNA also triggered DDR signalling as judged by elevated CHK2 and p53 phosphorylation (Fig. 5C).

To probe whether DDR signalling was increased as a consequence of elevated DNA damage levels, we next examined DSB formation by co-labelling for the DNA repair mediators γH2AX and 53BP1 (Fig. 5D), revealing that the number of cells with more than five DSBs per cell increased three-fold upon MOB2 silencing (Fig. 5E). The accumulation of DSBs was proliferation dependent, as hMOB2 depletion had no effect in non-cycling cells (Fig. 5F and G). Proliferating hMOB2-depleted cells displayed activation of ATM–CHK2–p53–p21 signalling, while controls and serum-starved cells did not (Fig. 5H), indicating that hMOB2 depletion triggers activation of the ATM–p53–p21 cascade. Next, we

Fig. 5. In normal growth conditions hMOB2-depleted cells accumulate unrepaired DNA damage, triggering ATM–p53–p21 signalling. (A, B) Immunoblotting of RPE1 Tet-on shMOB2 cell lysates from cells incubated with (+Tet) or without (−Tet) tetracycline for indicated times. Controls were incubated with doxorubicin (+Dox). (C) Immunoblotting of RPE1, MCF10A, and BJ cell lysates from cells transiently transfected with indicated siRNAs. (D) Immunodetection of 53BP1 (green) and γH2AX (red) in RPE1 Tet-on shMOB2 cells grown in the presence (+Tet) or absence (−Tet) of tetracycline for 96 h. DNA is stained blue. (E) Histograms showing percentages of cells with DSBs in the presence of serum. Only cells displaying at least (≥) 5 double positive 53BP1/γH2AX DSB foci per nuclei were counted as DSB positive (1000 cells per time point in control (grey) or hMOB2-depleted (black) cells (P-value = 0.006). (F) Immunodetection of 53BP1 (green) and γH2AX (red) in RPE1 Tet-on shMOB2 cells cultured in the presence (+Tet) or absence (−Tet) of tetracycline without serum (0% FCS) for 96 h. (G) Histograms showing percentages of cells with DSBs in the absence of serum. Cells were scored as described in E. (H) Immunoblotting of RPE1 Tet-on shMOB2 cell lysates from cells serum-starved for 72 h with (+Tet) or without (−Tet) tetracycline, before addition of medium without (0% FBS) or with serum (10% FBS) for another 72 h. (I) Measurement of DNA breaks by comet assays in RPE1 Tet-on shMOB2 cells treated with (+Tet) or without (−Tet) tetracycline for 96 h. (J) Quantification of DNA damage by comet assay in RPE1 Tet-on shMOB2 cells at indicated time points (n = 3). P-values are: 48 h = 2.67E−03; 72 h = 1.69E−05; 96 h = 2.23E−20. IR at 15Gy served as positive control.

Please cite this article as: V. Gomez, et al., Cell. Signal. (2014), http://dx.doi.org/10.1016/j.cellsig.2014.11.016

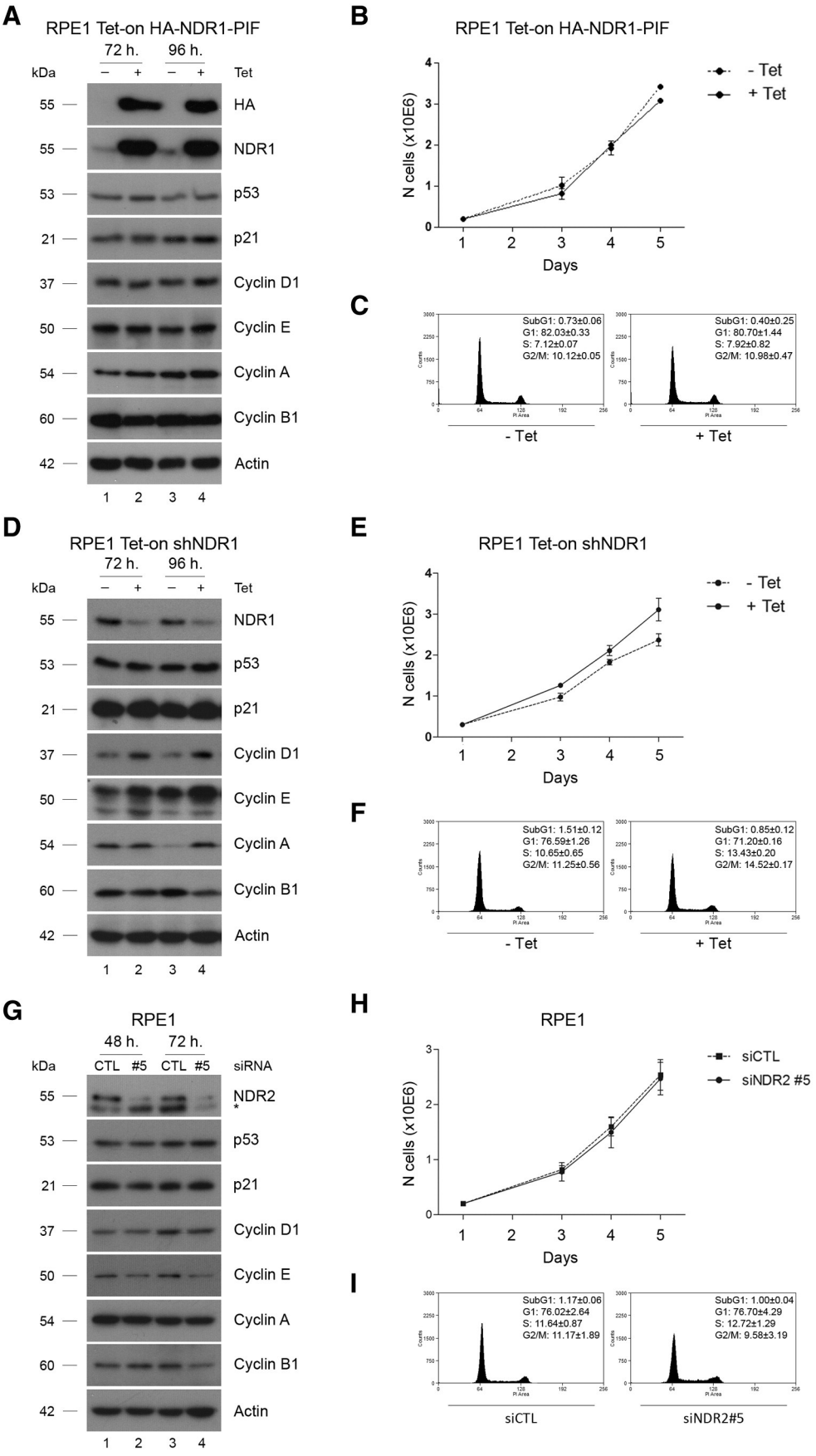
A
RPE1 Tet-on HA-NDR1-PIF
72 h.
96 h.
kDa
– + – +
Tet
55 HA
55 NDR1
53 p53
21 p21
37 Cyclin D1
50 Cyclin E
54 Cyclin A
60 Cyclin B1
42 Actin
1 2 3 4
B
RPE1 Tet-on HA-NDR1-PIF
N cells (x10E6)
Days
- Tet
+ Tet
C
SubG1: 0.73±0.06
G1: 82.03±0.33
S: 7.12±0.07
G2/M: 10.12±0.05
SubG1: 0.40±0.25
G1: 80.70±1.44
S: 7.92±0.82
G2/M: 10.98±0.47
- Tet
+ Tet
D
RPE1 Tet-on shNDR1
72 h.
96 h.
kDa
– + – +
Tet
55 NDR1
53 p53
21 p21
37 Cyclin D1
50 Cyclin E
54 Cyclin A
60 Cyclin B1
42 Actin
1 2 3 4
E
RPE1 Tet-on shNDR1
N cells (x10E6)
Days
- Tet
+ Tet
F
SubG1: 1.51±0.12
G1: 76.59±1.26
S: 10.65±0.65
G2/M: 11.25±0.56
SubG1: 0.85±0.12
G1: 71.20±0.16
S: 13.43±0.20
G2/M: 14.52±0.17
- Tet
+ Tet
G
RPE1
48 h.
72 h.
kDa
CTL #5 CTL #5
siRNA
55 NDR2 *
53 p53
21 p21
37 Cyclin D1
50 Cyclin E
54 Cyclin A
60 Cyclin B1
42 Actin
1 2 3 4
H
RPE1
N cells (x10E6)
Days
siCTL
siNDR2 #5
I
SubG1: 1.17±0.06
G1: 76.02±2.64
S: 11.64±0.87
G2/M: 11.17±1.89
SubG1: 1.00±0.04
G1: 76.70±4.29
S: 12.72±1.29
G2/M: 9.58±3.19
siCTL
siNDR2#5

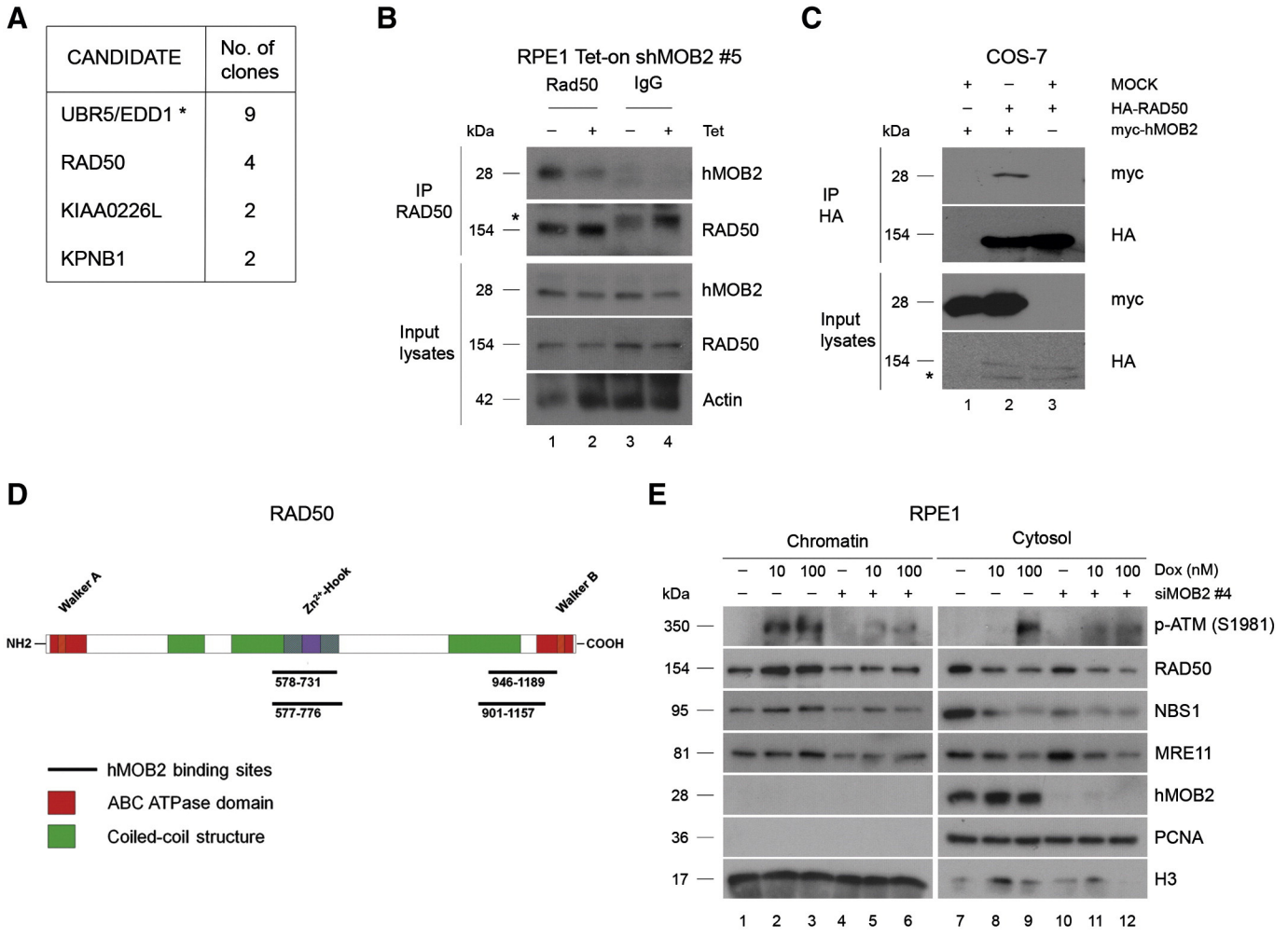

Fig. 7. hMOB2 interacts with the MRN component RAD50, regulating MRN–ATM recruitment to DNA damaged chromatin. (A) List of novel hMOB2 binding partners identified at least twice by yeast two-hybrid (Y2H) screens. The number of independent hits is indicated. (B) RPE1 Tet-on shMOB2 cells incubated with (+Tet) or without (−Tet) tetracycline for 96 h were subjected to immunoprecipitation (IP) using anti-RAD50 (RAD50) or control (IgG) antibodies, before inputs and immunoprecipitates were analysed by immunoblotting. Asterisk (*) marks an unspecific band in the RAD50 blot. (C) COS-7 lysates transiently expressing indicated combinations of HA-tagged RAD50 and myc-tagged hMOB2 were subjected to immunoprecipitation using anti-HA 12CA5 antibody, before immunoblotting of immuno-complexes and input lysates. (D) Primary structure of RAD50 indicating direct hMOB2 binding sites defined by Y2H mapping. Known functional domains of RAD50 are highlighted. (E) RPE1 cells transiently transfected for 24 h with indicated siRNAs (−, siCTL; +, siMOB2) were treated with indicated doxorubicin doses, before separation into chromatin and cytosolic fractions, and subsequent immunoblotting with indicated antibodies.

performed comet assays to measure DNA breakage directly, revealing that upon hMOB2 depletion cells rapidly accumulate DNA breaks (Fig. 5I and J). Significantly, this analysis further showed that in hMOB2-depleted cells DNA breakage was elevated before DSBs were detectable by immunofluorescence (compare Fig. 5E and J). Since γH2AX/53BP1 accumulates at DSBs only after DDR activation [43], these findings indicate that DNA lesions precede DDR activation in hMOB2-depleted cells. Collectively, these data show that hMOB2 is required to prevent the accumulation of unrepaired DNA damage. Once hMOB2 levels are decreased, unrepaired DNA damage accumulates, triggering DNA damage-p53 signalling, which elevates p21 expression to arrest cells at the G1/S cell cycle checkpoint.

3.5. Neither NDR manipulations nor hMOB2 overexpression halt cell cycle progression

p53 stabilisation/activation can occur via a variety of distinct mechanisms [50]. Considering that NDR is the only reported binding partner of hMOB2 [1], we interrogated NDR signalling as a possible mechanism. We speculated that hMOB2 depletion might cause hypo- or hyperactivation of NDR signalling which potentially could help us to understand how hMOB2 depletion triggers a p53-dependent G1/S cell cycle arrest. To study the importance of NDR signalling in our settings, we pursued three different avenues. First, we generated and subsequently analysed cells with Tet-on inducible overexpression of constitutively hyperactive NDR1-PIF [38] to mimic possible hyperactivation of NDR upon hMOB2 depletion (Fig. 6A–C). Second, NDR1 and NDR2 kinases were depleted to mimic possible hypoactivation of NDR signalling in our settings (Fig. 6D–I). Third, we generated cells with Tet-on inducible overexpression of hMOB2 (Supplementary Fig. S3) to test whether hMOB2 functioning as an inhibitor of NDR kinases [18] plays a role in cell cycle progression. Unexpectedly, neither overexpression of hyperactive NDR1 nor NDR depletions negatively affected cell proliferation (Fig. 6). Moreover, hMOB2 overexpression did not alter cell proliferation (Supplementary Fig. S3). Therefore, we concluded that NDR signalling is not essential for p53-regulated proliferation of

Fig. 6. NDR signalling is not required for cell cycle progression of RPE1 cells. (A) Immunoblotting of RPE1 Tet-on HA-NDR1-PIF cell lysates from cells incubated with (+Tet) or without (−Tet) tetracycline for indicated times. (B) Proliferation rates of RPE1 Tet-on HA-NDR1-PIF cells (n = 3). (C) Cell cycle analyses of RPE1 Tet-on HA-NDR1-PIF cells after 96 h in the presence (+Tet) or absence (−Tet) of tetracycline (n = 3). (D) Immunoblotting of RPE1 Tet-on shNDR1#4 cell lysates as described in A. (E) Proliferation rates of RPE1 Tet-on shNDR1#4 cells (n = 3). (F) Cell cycle analyses of RPE1 Tet-on shNDR1#4 cells after 96 h in the presence (+Tet) or absence (−Tet) of tetracycline (n = 3). (G) Immunoblotting of RPE1 cell lysates from cells transfected with indicated siRNAs (CTL, control; #5, siNDR2). Asterisk (*) in NDR2 blot marks an unspecific band. (H) Proliferation rates of indicated cell lines (n = 3). (I) Cell cycle analyses of RPE1 cells 96 h after indicated siRNA transfections (n = 3).

untransformed RPE1 cells. Evaluated in a broader context together with the findings described in Figs. 3 and 4, these observations further indicate that endogenous hMOB2 is required for normal cell cycle progression independent of NDR kinase signalling.

3.6. hMOB2 interacts with RAD50, regulating MRN–ATM recruitment to DNA damaged chromatin

To uncover how hMOB2 can function as a DDR protein, we performed yeast two hybrid (Y2H) screens with full-length hMOB2 as a bait, aiming to identify novel direct (binary) binding partners of hMOB2 that are linked to DDR signalling (Supplementary Table S1). Significantly, this screen revealed UBR5 and RAD50, two known DDR proteins, as top candidates (Fig. 7A). The HECT domain E3 ligase UBR5 (also termed EDD1) was the most frequently isolated prey (Fig. 7A and Supplementary Table S1). However, all hits for UBR5 were not in frame with the GAL4 activation domain (Supplementary Table S1), and the interaction between hMOB2 and UBR5 was undetectable by co-immunoprecipitation experiments upon overexpression in mammalian cells (Supplementary Fig. S4). This indicates that the observed Y2H interaction between hMOB2 and UBR5 is very likely an Y2H artefact. Furthermore, UBR5 knockdown affects IR-induced KAP1 phosphorylation, without altering ATM autophosphorylation [53], and impairs DNA damage-induced CHK2 phosphorylation [54]. Moreover, UBR5 overexpression inhibits p53 phosphorylation by ATM [55]. Therefore, as IR-induced KAP1, CHK2, and p53 phosphorylation were unaffected in hMOB2-depleted cells (Fig. 2), it is very unlikely that hMOB2 is relevant for UBR5 function.

Consequently, we focused on understanding the interaction between hMOB2 and RAD50, which was repeatedly observed by Y2H (Fig. 7A). RAD50 is a key component of the MRN complex, which is required from DNA damage detection to triggering DDR signalling, subsequently activating cell cycle checkpoints and DNA repair pathways [26–28]. Thus, the identification of novel MRN regulators has insightful implications for our understanding of the DDR in human cell biology [25]. Moreover, a link between hMOB2 and MRN function could explain why hMOB2-depleted cells display heightened sensitivity to DNA damaging agents, impaired DDR signalling, defective cell cycle checkpoints, accumulation of unrepaired DNA damage, and a cell cycle progression defect. We first aimed to confirm the interaction of hMOB2 with RAD50 in mammalian cells. In contrast to our findings with regard to UBR5 (see Supplementary Fig. S4), co-immunoprecipitation experiments using mammalian cell lysates readily detected the formation of hMOB2/RAD50 complexes on endogenous and exogenous levels (Fig. 7B and C). Furthermore, Y2H mapping defined the region surrounding the zinc hook domain and a C-terminal stretch encompassing part of the ABC domain of RAD50 as binary binding sites for hMOB2 (Fig. 7D).

Given this novel and unexpected link between hMOB2 and MRN through the hMOB2/RAD50 interaction, we wondered whether hMOB2 contributes to DNA damage induced chromatin binding of MRN and subsequent ATM recruitment, which is crucial for efficient MRN-mediated ATM signalling [26–28]. To avoid indirect cell cycle effects in our analysis of MRN functionality, we examined cells 24 h after siRNA transfection, since at this time point neither MRN was decreased nor p53 levels were increased despite efficient hMOB2 depletion (Supplementary Fig. S5). To induce DNA damage exogenously, cells were treated with doxorubicin, before cells were subjected to chromatin–cytosol fractionations, followed by immunoblotting of MRN to detect DNA damage-induced enrichment at chromatin. Significantly, this analysis revealed that hMOB2 is required for normal MRN recruitment to DNA damaged chromatin, since DNA damage-induced enrichment of MRN at chromatin was severely impaired upon hMOB2 depletion (Fig. 7E). In addition, enrichment of activated ATM at DNA damaged chromatin was also dependent on hMOB2 (Fig. 7E, top panel). Similar results were obtained when hMOB2 was depleted by an independent shRNA using RPE1 Tet-on shMOB2 cells (data not shown). Taken together, these findings indicate that hMOB2 supports the recruitment of MRN and activated ATM to DNA damaged chromatin, hence providing the first mechanistic insight into how hMOB2 can contribute to optimal ATM activation and ATM substrate phosphorylation.

4. Discussion

We describe herein novel functions of hMOB2 in the DDR and cell cycle regulation. Like MRN deficient cells [26–28], hMOB2-depleted cells display impaired cell proliferation, heightened sensitivity to DNA damaging agents, defective cell cycle checkpoints, and suboptimal ATM activation. Therefore, our data cumulatively suggest that hMOB2 supports MRN functionality, which is crucial for DNA damage detection, DDR signalling, and cell cycle checkpoint activation, consequently promoting efficient DNA repair. Hypothetically, impaired ATM activation could result from ATMIN deficiency, another ATM activator [56]. However, unlike ATMIN deficiency [56], hMOB2 depletion decreased IR-induced SMC1 phosphorylation and increased radiosensitivity, indicating hMOB2 knockdown does not phenocopy ATMIN deficiency. Our data rather advocate that MRN functionality is impaired in hMOB2-depleted cells, since MRN retention at DNA damaged chromatin is defective, MRN-mediated recruitment of activated ATM to DNA damaged chromatin is reduced, hence IR-induced ATM activation is impaired, and ATM-mediated NBS1 and SMC1 phosphorylation decreases. Collectively, our data show that hMOB2 depletion mimics certain aspects of MRN deficiency on the molecular and cellular level.

Our data provide the first mechanistic insight into how hMOB2 can function in the DDR by suggesting that hMOB2 contributes to the DDR on at least two molecular levels. On the one hand, hMOB2 contributes to MRN-mediated recruitment of activated ATM to DNA damaged chromatin. On the other hand, hMOB2 seems to support MRN as an adaptor for ATM substrates such as SMC1, while hMOB2 is dispensable for IR-induced ATM-mediated phosphorylation of p53 and CHK2. These findings suggest that hMOB2 is required to promote MRN-mediated signalling events, while hMOB2 is expendable for MRN-independent ATM signalling. This interpretation is in full agreement with published reports showing that SMC1 phosphorylation by ATM is MRN-dependent [46–48] and defective ATM activation is quantitative, not absolute, in MRN mutant cells [47,57–59], while MRN-mediated ATM activation is dispensable for CHK2 and p53 phosphorylation [60,61]. Moreover, our data suggest that the observed suboptimal activation of ATM is a consequence of impaired MRN functionality due to hMOB2 depletion. This conclusion is fully supported by previous reports demonstrating that the positive feedback loop maintaining optimal ATM activation requires MRN-mediated ATM recruitment to damaged DNA [45]. Decreased ATM-mediated SMC1 and NBS1 phosphorylation could result from defective MRN-ATM recruitment to DNA damaged chromatin upon hMOB2 depletion. Conversely, these signalling events could represent separate, but interlinked, MRN functions supported by hMOB2. Possibly, hMOB2 is also required for efficient ATM phosphorylation of other substrates, besides NBS1 and SMC1, since ATM has potentially more than 700 substrates [45]. Therefore, since MRN exists in diverse conformational and assembly states [26,28], future structural and biochemical studies are warranted to further dissect hMOB2 as facilitator of MRN recruitment to DNA damaged chromatin and as an adaptor for ATM substrates. Particular attention will be paid to dissecting the RAD50/hMOB2 interaction in the context of our Y2H mapping data and the unique architecture of RAD50, which is essential to support MRE11/RAD50 binding to DNA via MRE11's DNA binding motifs and RAD50's ABC domains, while DNA break tethering is achieved through RAD50's zinc hook domain supported by RAD50's coiled-coil structure [26–28].

MRN is also required for balanced DSB repair [26–28]. Misbalance between DNA damage and repair results in higher p53 levels through pulses [62], causing a transient p53-dependent G1/S cell cycle arrest [51]. Similarly, under normal growth conditions in the absence of

Please cite this article as: V. Gomez, et al., Cell. Signal. (2014), http://dx.doi.org/10.1016/j.cellsig.2014.11.016

exogenously induced DNA damage, hMOB2-depleted cells accumulate unrepaired DNA damage, triggering a p53-dependent G1/S cell cycle arrest. Thus, our findings collectively suggest that the roles of hMOB2 in the DDR and cell cycle progression are interlinked, proposing the following working model for normal growth conditions: generally, low endogenous DNA damage (as normally caused by reactive oxygen species, DNA replication, and other mechanisms [63]) is sensed by the MRN to coordinate the necessary DDR steps. In contrast, hMOB2-depletion impairs MRN recruitment to DNA damaged chromatin. Consequently endogenous DNA damage is detected inefficiently, causing accumulation of DNA damage, which triggers a p53-dependent G1/S arrest in hMOB2-depleted cells under normal growth conditions without exogenously induced DNA damage.

Upon exposure to high levels of exogenously induced DNA damage hMOB2 is further needed to promote activation of the G1/S and G2/M cell cycle checkpoints. We report here a defective G1/S checkpoint in hMOB2-depleted cells upon exposure to high DNA damage levels, and Cotta-Ramusino et al. showed that hMOB2-depleted cells have impaired activation of the IR-induced G2/M cell cycle checkpoint [24]. Most likely, these DDR cell cycle checkpoint defects are a result of impaired MRN functionality upon hMOB2 depletion, since we show here that hMOB2 is needed to support MRN functionality and MRN deficiencies are known to weaken the G1/S and G2/M cell cycle checkpoints [26–28]. Notably, given that cell survival in response to DNA damage relies on proper cell cycle control, these cell cycle checkpoint interpretations can also help to explain why hMOB2 contributes to cell survival upon exposure to different DNA damaging agents. Nevertheless, we have only begun to understand how hMOB2 promotes cell survival and cell cycle checkpoint activation upon exposure to DNA damage, hence future studies into the regulation and wiring of cell cycle checkpoints by hMOB2 are warranted.

The human *MOB2* gene appears to display LOH in more than 50% of bladder, cervical and ovarian carcinomas (TCGA) [21], hence, hMOB2 might represent a novel tumour suppressor promoting the DDR response. Future studies are therefore warranted to explore in yet to be developed animal models the consequences of MOB2 deficiency for tumour formation and the response to DNA damaging treatments. Considering that at least 30% of cancer cell lines [21] seem to display LOH of the *MOB2* gene, tissue culture approaches may be able to initially complement these upcoming experiments. Although hMOB2 is unlikely to serve as good drug target, future studies are also needed to investigate whether hMOB2 expression may offer a means to stratify patients for DNA damaging therapies, with the aim of potentially reducing the frequency of cancer therapy resistance [64], in addition to further expanding our understanding of the role of hMOB2 in human cell biology and disease.

5. Conclusions

In summary, our study provides, for the first time, evidence suggesting that hMOB2 is a novel DDR protein. In normal growth conditions hMOB2 is required to prevent the accumulation of unrepaired DNA damage. Upon exposure to high levels of exogenously induced DNA damage hMOB2 supports cell survival, cell cycle checkpoint activation, and DDR signalling. Surprisingly, these novel functions of hMOB2 appear to be independent of NDR signalling, but rather seem to be dependent on a link between hMOB2 and the MRN DNA damage sensor complex, since hMOB2 supports the recruitment of MRN and activated ATM to DNA damaged chromatin. Consequently, we provide novel insights into signalling functions of hMOB2 that possibly are critical in human diseases linked to DDR defects.

Conflict of interest

The authors declare that they have no conflict of interest.

Acknowledgements

We thank J. Lisztwan and H. Yamano for critical reading of the manuscript. We further thank V. Spanswick (UCL Cancer Institute) for kindly assisting in establishing comet assays. RAD50 cDNA and BJ fibroblasts were a gift from C. Wyman (Erasmus University Medical Center, Rotterdam, The Netherlands) and T. Waldman (Lombardi Cancer Center, Washington, USA), respectively. VG was supported by AICR (11-0634). RG is sponsored by the Ministry of National Education (The Republic of Turkey). This work was further supported by BBSRC (BB/I021248/1), Wellcome Trust (090090/Z/09/Z), and the National Institute for Health Research University College London Hospitals Biomedical Research Centre. AH is a Wellcome Trust Research Career Development fellow at the UCL Cancer Institute.

Appendix A. Supplementary data

Supplementary data to this article can be found online at http://dx.doi.org/10.1016/j.cellsig.2014.11.016.

References

[1] A. Hergovich, Cell. Signal. 23 (2011) 1433–1440.
[2] M. Hotz, Y. Barral, Trends Cell Biol. 24 (2014) 145–152.
[3] A.E. Johnson, D. McCollum, K.L. Gould, Cytoskeleton. (Hoboken) 69 (2012) 686–699.
[4] F. Meitinger, S. Palani, G. Pereira, Cell Cycle 11 (2012) 219–228.
[5] K.F. Harvey, X. Zhang, D.M. Thomas, Nat. Rev. Cancer 13 (2013) 246–257.
[6] Z.C. Lai, X. Wei, T. Shimizu, E. Ramos, M. Rohrbaugh, N. Nikolaidis, L.L. Ho, Y. Li, Cell 120 (2005) 675–685.
[7] B.K. Staley, K.D. Irvine, Dev. Dyn. 241 (2012) 3–15.
[8] M.E. Campbell, B.S. Ganetzky, Identification of Mob2, a Novel Regulator of Larval Neuromuscular Junction Morphology, in Natural Populations of Drosophila melanogaster, Genetics, 2013.
[9] L.Y. Liu, C.H. Lin, S.S. Fan, Cell Tissue Res. 338 (2009) 377–389.
[10] Y. He, K. Emoto, X. Fang, N. Ren, X. Tian, Y.N. Jan, P.N. Adler, Mol. Biol. Cell 16 (2005) 4139–4152.
[11] W. Geng, B. He, M. Wang, P.N. Adler, Genetics 156 (2000) 1817–1828.
[12] J. Avruch, D. Zhou, J. Fitamant, N. Bardeesy, F. Mou, L.R. Barrufet, Semin. Cell Dev. Biol. 23 (2012) 770–784.
[13] A. Hergovich, Cell Biosci. 3 (2013) 32.
[14] M. Nishio, K. Hamada, K. Kawahara, M. Sasaki, F. Noguchi, S. Chiba, K. Mizuno, S.O. Suzuki, Y. Dong, M. Tokuda, et al., J. Clin. Invest. 122 (2012) 4505–4518.
[15] A. Hergovich, M.R. Stegert, D. Schmitz, B.A. Hemmings, Nat. Rev. Mol. Cell Biol. 7 (2006) 253–264.
[16] J. Bothos, R.L. Tuttle, M. Ottey, F.C. Luca, T.D. Halazonetis, Cancer Res. 65 (2005) 6568–6575.
[17] A. Hergovich, D. Schmitz, B.A. Hemmings, Biochem. Biophys. Res. Commun. 345 (2006) 50–58.
[18] R.S. Kohler, D. Schmitz, H. Cornils, B.A. Hemmings, A. Hergovich, Mol. Cell. Biol. 30 (2010) 4507–4520.
[19] A. Hergovich, R.S. Kohler, D. Schmitz, A. Vichalkovski, H. Cornils, B.A. Hemmings, Curr. Biol. 19 (2009) 1692–1702.
[20] F. Tang, L. Zhang, G. Xue, D. Hynx, Y. Wang, P.D. Cron, C. Hundsrucker, A. Hergovich, S. Frank, B.A. Hemmings, et al., HMOB3 modulates MST1 apoptotic signaling and supports tumor growth in glioblastoma multiform, Cancer Res, 2014.
[21] E. Cerami, J. Gao, U. Dogrusoz, B.E. Gross, S.O. Sumer, B.A. Aksoy, A. Jacobsen, C.J. Byrne, M.L. Heuer, E. Larsson, et al., Cancer Discov. 2 (2012) 401–404.
[22] K.M. Fang, Y.Y. Liu, C.H. Lin, S.S. Fan, C.H. Tsai, S.F. Tzeng, J. Cell. Biochem. 113 (2012) 3019–3028.
[23] C.H. Lin, M. Hsieh, S.S. Fan, FEBS Lett. 585 (2011) 523–530.
[24] C. Cotta-Ramusino, E.R. McDonald 3rd, K. Hurov, M.E. Sowa, J.W. Harper, S.J. Elledge, Science 332 (2011) 1313–1317.
[25] S.P. Jackson, J. Bartek, Nature 461 (2009) 1071–1078.
[26] A. Rupnik, N.F. Lowndes, M. Grenon, Chromosoma 119 (2010) 115–135.
[27] T.H. Stracker, J.H. Petrini, Nat. Rev. Mol. Cell Biol. 12 (2011) 90–103.
[28] G.J. Williams, S.P. Lees-Miller, J.A. Tainer, DNA Repair (Amst) 9 (2010) 1299–1306.
[29] J. Debnath, S.K. Muthuswamy, J.S. Brugge, Methods 30 (2003) 256–268.
[30] M. Gomez-Martinez, D. Schmitz, A. Hergovich, J. Vis. Exp. (2013) e50171.
[31] M. van de Wetering, I. Oving, V. Muncan, M.T. Pon Fong, H. Brantjes, D. van Leenen, F.C. Holstege, T.R. Brummelkamp, R. Agami, H. Clevers, EMBO Rep. 4 (2003) 609–615.
[32] A. Hergovich, S. Lamla, E.A. Nigg, B.A. Hemmings, Mol. Cell 25 (2007) 625–634.
[33] A. Hergovich, S.J. Bichsel, B.A. Hemmings, Mol. Cell. Biol. 25 (2005) 8259–8272.
[34] H. Cornils, R.S. Kohler, A. Hergovich, B.A. Hemmings, Mol. Cell. Biol. 31 (2011) 1382–1395.
[35] A. Vichalkovski, E. Gresko, H. Cornils, A. Hergovich, D. Schmitz, B.A. Hemmings, Curr. Biol. 18 (2008) 1889–1895.
[36] P.L. Olive, J.P. Banath, Nat. Protoc. 1 (2006) 23–29.
[37] N.A. Franken, H.M. Rodermond, J. Stap, J. Haveman, C. van Bree, Nat. Protoc. 1 (2006) 2315–2319.

Please cite this article as: V. Gomez, et al., Cell. Signal. (2014), http://dx.doi.org/10.1016/j.cellsig.2014.11.016

[38] D. Cook, L.Y. Hoa, V. Gomez, M. Gomez, A. Hergovich, Cell. Signal. 26 (2014) 1657–1667.
[39] A.A. Sartori, C. Lukas, J. Coates, M. Mistrik, S. Fu, J. Bartek, R. Baer, J. Lukas, S.P. Jackson, Nature 450 (2007) 509–514.
[40] P. Bouwman, J. Jonkers, Nat. Rev. Cancer 12 (2012) 587–598.
[41] I.N. Colaluca, D. Tosoni, P. Nuciforo, F. Senic-Matuglia, V. Galimberti, G. Viale, S. Pece, P.P. Di Fiore, Nature 451 (2008) 76–80.
[42] M.B. Kastan, J. Bartek, Nature 432 (2004) 316–323.
[43] S.E. Polo, S.P. Jackson, Genes Dev. 25 (2011) 409–433.
[44] C.J. Bakkenist, M.B. Kastan, Nature 421 (2003) 499–506.
[45] Y. Shiloh, Y. Ziv, Nat. Rev. Mol. Cell Biol. 14 (2013) 197–210.
[46] S.T. Kim, B. Xu, M.B. Kastan, Genes Dev. 16 (2002) 560–570.
[47] R. Kitagawa, C.J. Bakkenist, P.J. McKinnon, M.B. Kastan, Genes Dev. 18 (2004) 1423–1438.
[48] P.T. Yazdi, Y. Wang, S. Zhao, N. Patel, E.Y. Lee, J. Qin, Genes Dev. 16 (2002) 571–582.
[49] C.R. Stumpf, M.V. Moreno, A.B. Olshen, B.S. Taylor, D. Ruggero, Mol. Cell 52 (2013) 574–582.
[50] J.P. Kruse, W. Gu, Cell 137 (2009) 609–622.
[51] J.E. Purvis, K.W. Karhohs, C. Mock, E. Batchelor, A. Loewer, G. Lahav, Science 336 (2012) 1440–1444.
[52] J.S. Kim, C. Lee, C.L. Bonifant, H. Ressom, T. Waldman, Mol. Cell. Biol. 27 (2007) 662–677.
[53] T. Gudjonsson, M. Altmeyer, V. Savic, L. Toledo, C. Dinant, M. Grofte, J. Bartkova, M. Poulsen, Y. Oka, S. Bekker-Jensen, et al., Cell 150 (2012) 697–709.
[54] M.J. Henderson, M.A. Munoz, D.N. Saunders, J.L. Clancy, A.J. Russell, B. Williams, D. Pappin, K.K. Khanna, S.P. Jackson, R.L. Sutherland, et al., J. Biol. Chem. 281 (2006) 39990–40000.
[55] S. Ling, W.C. Lin, J. Biol. Chem. 286 (2011) 14972–14982.
[56] N. Kanu, A. Behrens, Embo J. 26 (2007) 2933–2941.
[57] R. Waltes, R. Kalb, M. Gatei, A.W. Kijas, M. Stumm, A. Sobeck, B. Wieland, R. Varon, Y. Lerenthal, M.F. Lavin, et al., Am. J. Hum. Genet. 84 (2009) 605–616.
[58] T. Uziel, Y. Lerenthal, L. Moyal, Y. Andegeko, L. Mittelman, Y. Shiloh, Embo J. 22 (2003) 5612–5621.
[59] J.W. Theunissen, M.I. Kaplan, P.A. Hunt, B.R. Williams, D.O. Ferguson, F.W. Alt, J.H. Petrini, Mol. Cell 12 (2003) 1511–1523.
[60] T.H. Stracker, M. Morales, S.S. Couto, H. Hussein, J.H. Petrini, Nature 447 (2007) 218–221.
[61] D.S. Lim, S.T. Kim, B. Xu, R.S. Maser, J. Lin, J.H. Petrini, M.B. Kastan, Nature 404 (2000) 613–617.
[62] A. Loewer, E. Batchelor, G. Gaglia, G. Lahav, Cell 142 (2010) 89–100.
[63] T. Lindahl, D.E. Barnes, Cold Spring Harb. Symp. Quant. Biol. 65 (2000) 127–133.
[64] C. Holohan, S. Van Schaeybroeck, D.B. Longley, P.G. Johnston, Nat. Rev. Cancer 13 (2013) 714–726.

Please cite this article as: V. Gomez, et al., Cell. Signal. (2014), http://dx.doi.org/10.1016/j.cellsig.2014.11.016